

A gene encoding a putative GTPase regulator is mutated in familial amyotrophic lateral sclerosis 2

Shinji Hadano^{1,2}, Collette K. Hand³, Hitoshi Osuga^{1,2}, Yoshiko Yanagisawa¹, Asako Otomo¹, Rebecca S. Devon⁴, Natsuki Miyamoto¹, Junko Showguchi-Miyata², Yoshinori Okada², Roshni Singaraja⁴, Denise A. Figlewicz⁵, Thomas Kwiatkowski⁶, Betsy A. Hosler⁶, Tally Sagie⁷, Jennifer Skaug⁸, Jamal Nasir^{4,9}, Robert H. Brown, Jr⁶, Stephen W. Scherer⁸, Guy A. Rouleau³, Michael R. Hayden⁴ & Joh-E Ikeda^{1,2,10}

Amyotrophic lateral sclerosis 2 (ALS2) is an autosomal recessive form of juvenile ALS and has been mapped to human chromosome 2q33. Here we report the identification of two independent deletion mutations linked to ALS2 in the coding exons of the new gene ALS2. These deletion mutations result in frameshifts that generate premature stop codons. ALS2 is expressed in various tissues and cells, including neurons throughout the brain and spinal cord, and encodes a protein containing multiple domains that have homology to RanGEF as well as RhoGEF. Deletion mutations are predicted to cause a loss of protein function, providing strong evidence that ALS2 is the causative gene underlying this form of ALS.

Introduction

Amyotrophic lateral sclerosis (ALS) is a heterogeneous group of inexorable neurodegenerative disorders characterized by a selective loss of upper and lower motor neurons in the brain and spinal cord¹. Although most cases reported are sporadic (SALS), 5–10% are familial (FALS). Five types of FALS have been assigned to the distinct loci of the human genome. The gene for an autosomal dominant form with late onset (*ALS1*) maps to chromosome 21q22.1–q22.2 (ref. 2) and is associated with missense mutations in the copper–zinc superoxide dismutase gene (*SOD1*)³. A dominant form of juvenile ALS (ALS4) has been mapped to chromosome 9q34 (refs. 4,5). Two types of autosomal recessive forms for juvenile ALS, ALS2 and ALS5, have been mapped to chromosomes 2q33 (refs. 6,7) and 15q15–q22 (ref. 8), respectively. In addition, an autosomal dominant form of ALS with frontotemporal dementia (ALS-FTD) has recently been assigned to chromosome 9q21–q22 (ref. 9). Pedigrees with adult-onset, autosomal-dominant ALS that is neither linked to chromosome 21 nor associated with *SOD1* mutations suggest an additional locus for FALS, which is currently called *ALS3* (ref. 2). These data indicate the genetic heterogeneity of FALS, for which all genetic causes except *ALS1* are still unknown. To delineate the molecular pathogenesis of ALS and other motor-neuron diseases, identification of additional genes and their mutations that link to FALS is essential.

The disorder ALS2 (OMIM 205100), also known as type 3 autosomal recessive ALS (RFALS type 3), was originally reported in a large consanguineous Tunisian kindred and was characterized by a loss of upper motor neurons and spasticity of limb and facial muscles accompanying distal amyotrophy of hands and feet¹⁰. The *ALS2* locus has been mapped by linkage and haplotype analyses to the 1.7-cM interval flanked by *D2S116* and *D2S2237* (refs. 6,7). YAC-, BAC- and PAC-based physical cloning and mapping have shown that this interval spans approximately 3 Mb of genomic DNA^{7,11,12} and have allowed the generation of a transcript map of the *ALS2* critical region. Within this interval, several candidate genes for ALS2 have been assigned^{7,11,12}. A recent study showed that no sequence alterations associated with *ALS2* have been found in four exons encoding *CD28* and three exons encoding *CTLA4*, indicating that *CD28* and *CTLA4* are not causative genes for ALS2 (ref. 7). Despite such substantial studies, the genetic cause underlying ALS2 has yet to be identified.

We have identified 42 nonoverlapping transcripts within the *ALS2* candidate interval^{11,12} and searched the disease-associated DNA sequence for alterations in 395 exons and their flanking regions derived from these genes. We found two independent deletion mutations in the coding exons of a new gene, *ALS2* (initially identified as *ALS2CR6*), in the Tunisian and Kuwaiti ALS2 families. These deletion mutations result in frameshifts that generate premature stop codons. We have also isolated the mouse

¹NeuroGenes, International Cooperative Research Project, Japan Science and Technology Corporation, Tokai University School of Medicine, Isehara, Kanagawa 259-1193, Japan. ²Department of Molecular Neuroscience, The Institute of Medical Sciences, Tokai University, Isehara, Kanagawa, Japan. ³Centre for Research in Neuroscience, McGill University, and Montreal General Hospital Research Institute, Montreal, Quebec, Canada. ⁴Department of Medical Genetics, and Centre for Molecular Medicine and Therapeutics, University of British Columbia and Children's and Women's Hospital, Vancouver, British Columbia, Canada. ⁵Departments of Neurology and Neurobiology & Anatomy, University of Rochester Medical Center, Rochester, New York, USA. ⁶Day Neuromuscular Research Laboratory, Navy Yard, Charlestown, Massachusetts, USA. ⁷Pediatric Neurology and Metabolic Neurogenetic Clinic, E. Wolfson Medical Center, Holon, Israel. ⁸Sackler School of Medicine, Tel Aviv University, Tel Aviv, Israel. ⁹Department of Genetics, The Hospital for Sick Children, Toronto, Ontario, Canada. ¹⁰Division of Genomic Medicine, University of Sheffield, Royal Hallamshire Hospital, Sheffield, UK. ¹¹Department of Paediatrics, Faculty of Medicine, University of Ottawa, Ottawa, Ontario, Canada. Correspondence should be addressed to J.-E.I. (e-mail: joh-e@nga.med.u-tokai.ac.jp) or M.R.H. (e-mail: mrh@cmmmt.ubc.ca).

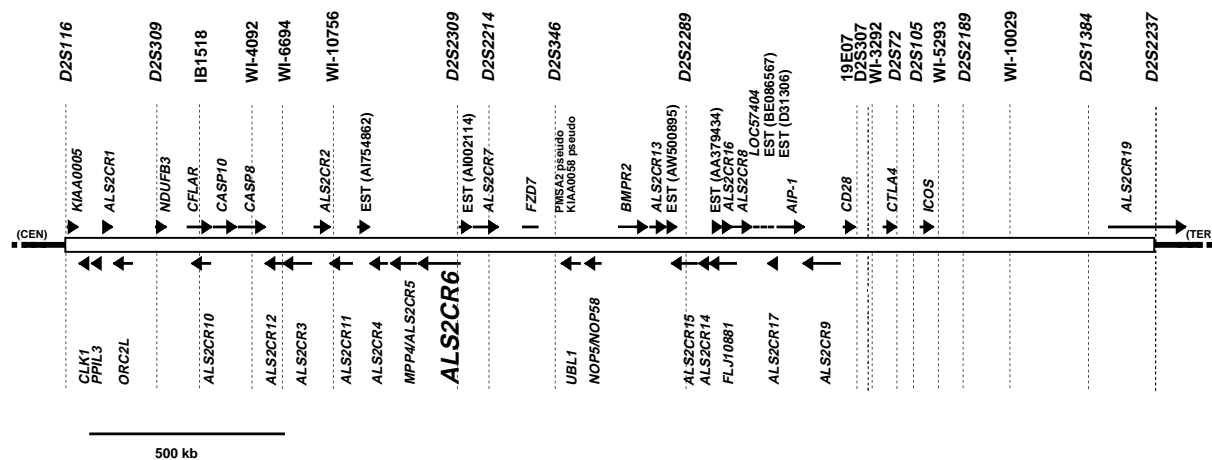


Fig. 1 A transcript map of the 3-Mb region of human chromosome 2q33 containing the *ALS2* candidate region. An open box spans the region between *D2S116* and *D2S2237*, which represents a critical region for the candidate interval for *ALS2* (ref. 7). Locations of 7 STS markers, 13 polymorphic DNA markers and 42 nonoverlapping transcriptional units are shown based on the previously reported physical map^{11,12}. Polarities of 38 transcriptional units are drawn as indicated as arrows.

ortholog for *ALS2* (*Als2*). Both transcripts are expressed in various tissues and cells, including neurons throughout the brain and spinal cord, and encode proteins containing several guanine-nucleotide exchange factor for Ran (RanGEF)¹³ and the guanine-nucleotide exchange factor for Rho (RhoGEF)¹⁴. Deletion mutations are predicted to abolish protein function, providing strong evidence that *ALS2* is the causative gene underlying *ALS2*.

Results

A transcript map and the *ALS2* candidate genes

We previously generated a YAC-, BAC-, and PAC-based physical map of the 3-Mb genomic region covering the complete candidate region for *ALS2* (refs. 11,12). Using this physical map, combined with extensive analyses of EST sequences and DNA sequencing of cDNA clones, we mapped 42 nonoverlapping transcriptional units, including 18 previously characterized genes (*KIAA0005*, *CLK1*, *PPIL3*, *ORC2L*, *NDUFB3*, *CFLAR*, *CASP10*, *CASP8*, *FZD7*, *UBL1*, *NOP5/NOP58*, *BMPR2*, *FLJ10881*, *LOC57404*, *AIP1*, *CD28*, *CTLA4* and *ICOS*) and 10 new full-length transcripts (*ALS2CR1*, *ALS2CR2*, *ALS2CR3*, *ALS2CR4*, *ALS2CR5*, *MPP4*, *ALS2CR6*, *ALS2CR7*, *ALS2CR8*, *ALS2CR9* and *ALS2CR12*; Fig. 1 and Web Table A).

Mutation detection in Tunisian family with *ALS2*

Juvenile *ALS2* is rare, and is heralded by symptoms in the first or second decade of life that include progressive spasticity of the limbs and the facial and pharyngeal muscles¹⁰. The recessive inheritance of *ALS2* led us to predict that the disease probably results from a loss-of-function mutation. We initially searched

for large deletions or rearrangements in the critical region in the Tunisian individuals with *ALS2* by PCR-based STS/EST content mapping and Southern blot analysis. We did not detect any evidence for such deletions or rearrangements (data not shown). We next screened for small deletions or base substitutions in exons or intron-exon boundaries. To identify these mutations, we analyzed the genomic organization of each transcript and defined the intron-exon boundaries for the candidate genes. We identified 395 exons derived from 42 candidate transcripts. Although not all the exons in the putative *ALS2* candidate interval are represented by these exons, the results of our extensive saturation mapping of transcripts suggests that the majority of exons are indeed included in this sample. We designed 411 pairs of primers to use in amplifying exons and their flanking sequences, including splicing donor and acceptor consensus sequences (Web Table B). We amplified exons and their flanking sequences from 14 Tunisian family members with *ALS2* (Fig. 2a) and 10 unrelated normal controls. By determining the DNA sequence for each PCR product, we identified a total of 77 sequence variations in either introns or exons (data not shown). Of these 77 variations, 6 intronic sequence variations and 2 exonic sequence changes are associated with the disease phenotype (Table 1) and haplotypes for adjacent DNA markers (data not shown).

Among these sequence changes, we observed a single-nucleotide deletion (261delA) in exon 3 of *ALS2CR6* that disrupts the reading frame and would be expected to have a deleterious effect on the encoded protein. All the suspected heterozygote carriers show a superimposed sequence pattern starting at the first nucleotide after the deletion (Fig. 2b). As this

Table 1 • Summary of sequence polymorphisms seen in Tunisian *ALS2* patients

Gene	Region	Normal	<i>ALS2</i>
<i>NOP5/NOP58</i>	intron 2	tatctc(T) ₉ aattct	→(T) ₆
<i>NOP5/NOP58</i>	intron 6	gttttg(TTG) ₂ ttttta	→(TTG) ₃
<i>ALS2CR6</i>	intron 2	ggtaaaAtcattt	→G
<i>ALS2CR6</i>	exon 3	gcaggcAgccctc	→ 261AdeI*
<i>ALS2CR8</i>	intron 6	gtcagtAttataa	→G
<i>ALS2CR9</i>	exon 4	ctccagCatggac	→ T (3rd codon)
<i>ALS2CR9</i>	intron 7	ttgggaTttttt	→A
<i>ALS2CR9</i>	intron 8	aaaataCgatgat	→I

ALS2-associated sequence variations are underscored. *denotes the mutation for the Tunisian *ALS2*.



261delA mutation generates a new *NarI* cutting site, we next carried out a mutation analysis using *NarI* to digest the exon 3 PCR products. The mutant allele produces two fragments of 225 bp and 113 bp in place of the 339-bp fragment representing the normal allele. We found that all the affected individuals studied carry a homozygous 261delA mutation, whereas all the predicted carriers show a heterozygous pattern (Fig. 2d); thus, the deletion co-segregates perfectly with the ALS2 phenotype. In addition, the 261delA mutation was not seen in 533 unrelated normal control individuals (61 North African individuals, whose racial background is the same as that of the family with ALS2; 94 Lebanese, whose ethnic origin overlaps with that of Tunisians; 310 Caucasians; and 68 Asians; data not shown). Other sequence changes (Table 1) include a C→T single-base substitution in exon 4 of *ALS2CR9* (C873T). This corresponds to the third codon and thus does not change the coding amino acid residue. To detect possible cryptic splicing or splicing errors resulting from other sequence variations, we carried out RT-PCR using total RNA samples extracted from lymphocytes of both affected patients and nor-

mal controls. We did not detect aberrant mRNA sequences (data not shown). Thus, it is likely that the single-base deletion (261delA) in *ALS2CR6* is the mutation underlying the Tunisian ALS2 phenotype.

Mutation detection in Kuwaiti family with ALS2

We also found a second truncating mutation in an unrelated family with ALS2 in Kuwait¹⁵ (Fig. 2a). Affected members of this family show early development of progressive spasticity with a

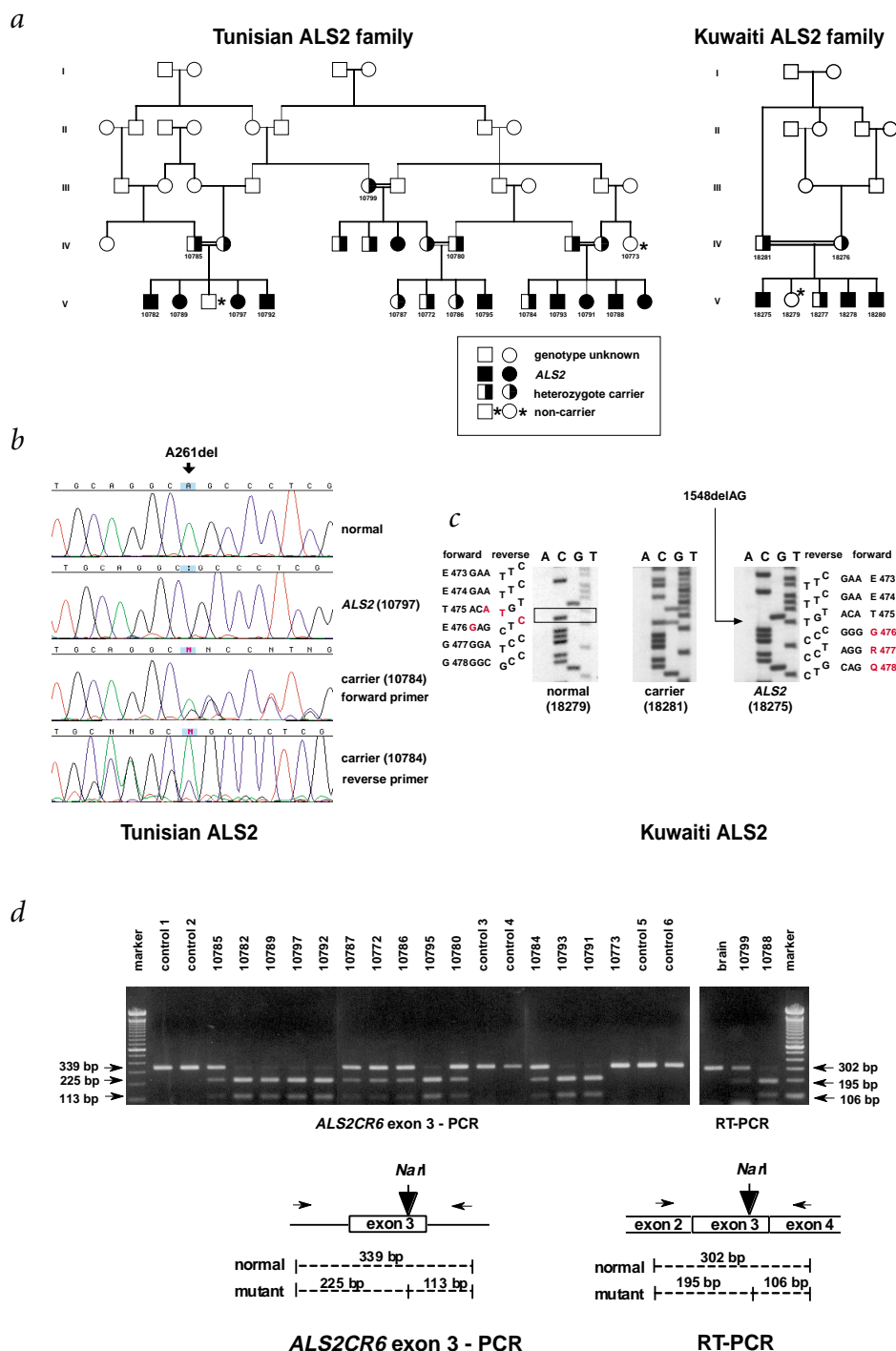


Fig. 2 Mutation detection in ALS2. **a**, A pedigree of the Tunisian and Kuwaiti families with ALS2. Genotypes of the family members were drawn based on reported^{6,7} and unpublished (Brown *et al.*) results. **b**, Sequence of the mutation (261delA) in the genomic DNA in the Tunisian ALS2 family. Patient 10797 is homozygous for 261delA, and carrier 10784 is heterozygous for the deletion. We carried out DNA sequencing of the products using both forward and reverse primers. **c**, Sequence of the mutation (1548delAG) in the genomic DNA in the Kuwaiti family with ALS2. Sequences of the reverse strand of exon 5 in the region of interest are shown. Individual 18279 is a normal sibling who is unaffected by ALS2 and carries two normal haplotypes. A box in this sequence indicates the position of the bases deleted (red letters) in affected members. Individual 18281 is an unaffected parent who carries one disease haplotype. The overlapping normal and mutated sequences can be clearly seen. Individual 18275 is affected; this sequence shows the homozygous CT deletion in the reverse strand of exon 5. The position of the deleted bases is indicated by the arrow. The corresponding forward sequence and coded normal amino acids (black) and novel amino acids produced by frameshifting (red) are indicated. **d**, Segregation of the 261delA mutation in the Tunisian family with ALS2. We assayed the presence of the deletion by digestion with *NarI*, which cuts only the mutant allele. On exon-PCR, the normal allele gives rise to a 339-bp fragment whereas the mutant allele gives rise to two fragments of 225 bp and 113 bp. On RT-PCR, the normal allele gives rise to a 302-bp product, whereas the mutant allele gives rise to two fragments of 195 bp and 106 bp.

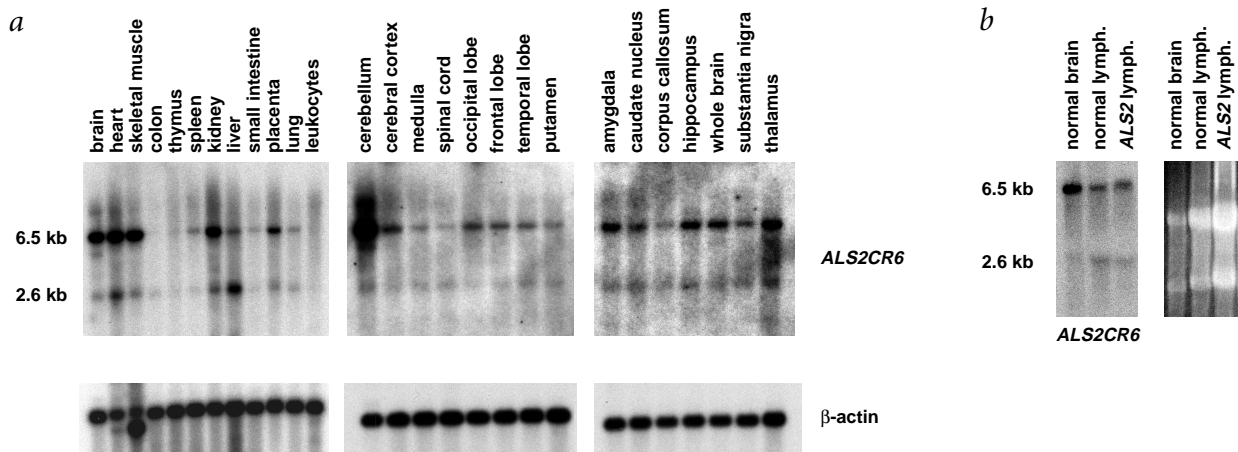


Fig. 3 Northern blot analysis of *ALS2* mRNA. **a**, We hybridized northern blots containing 2 μ g of poly(A)⁺ mRNA from various adult human tissues with exon 4 of the *ALS2* cDNA clone. The lower panel represents the same blots hybridized with the human β -actin cDNA to confirm RNA quality and relative loading. Sizes of the *ALS2* transcripts are shown on the left. **b**, Northern blots containing 10 μ g of total RNA from normal whole brain and 20 μ g of total RNA from lymphocytes derived from unaffected and affected (Tunisian; 10788) individuals were hybridized with exon 4 of the *ALS2* cDNA clone. The right panel represents the agarose gel electrophoresis of RNA samples.

time course and severity that resemble the clinical features as seen in the Tunisian family. However, in the Kuwaiti family, there was no evidence of denervation, at least in the first two decades of life. Haplotype analysis in this family confirms that the *ALS2* phenotype segregates perfectly with DNA markers for the 2q33 *ALS2* locus between *D2S116* and *D2S72*. The disease-associated haplotype in this *ALS2* kindred differs from that in the Tunisian family with *ALS2*, consistent with independent origins for the mutation (data not shown). We searched for DNA sequence variations in exons of *ALS2CR6* in five members of the Kuwaiti family (samples 18281, 18275, 18279, 18277 and 18278), and found a homozygous 2-bp deletion (1548delAG) in exon 5 of *ALS2CR6* in 2 affected individuals (18275 and 18278). Individuals carrying one disease haplotype are heterozygous for the deletion (18281 and 18277), whereas an unaffected individual carrying two normal haplotypes (18279) shows no deletion (Fig. 2c). The 1548delAG variation thus segregates perfectly with both disease phenotype and haplotypes for adjacent DNA markers. This deletion was not observed in a control group of 95 DNA samples of Arab descent, in 14 members of the Tunisian family with *ALS2* or in 10 normal Caucasian control DNA samples (data not shown). These findings suggest that the 1548AGdel is the causative mutation underlying the disease in this Kuwaiti family with *ALS2*.

Structure and expression of *ALS2*

The gene *ALS2CR6*, now officially designated *ALS2*, comprises 33 introns and 34 exons and resides within 80.3 kb of genomic DNA close to the polymorphic DNA marker *D2S2309* (Fig. 1; Web Table C). The transcriptional polarity of *ALS2* is in a telomere-to-centromere direction. The sequence of the *ALS2* transcript encompasses 6,394 nt with a single open reading frame (ORF; 4,974-nt long, nt 124–5,097), and is predicted to encode a 184-kD protein consisting of 1,657 amino acids. Putative polyadenylation signals (AATAAA; 6,375–6,380 nt) and a poly(A) tail are evident. Part of the *ALS2* sequence overlaps with that of the KIAA1563 cDNA clone¹⁶. We also identified a shorter transcript for *ALS2* that encompasses 2,651 nt with a single 1,191-nt ORF encoding 396 amino acids. This short variant was produced by alternate splicing at the 5' donor site after exon 4, resulting in a premature stop codon after 25 amino acid residues in intron 4. Consistent with these results, we identified by northern blotting

two transcripts of approximately 6.5 kb and 2.6 kb in various adult human tissues (Fig. 3a). Both transcripts show similar expression patterns, except in liver, where the shorter transcript is predominantly expressed. The 6.5-kb transcript is expressed at slightly higher levels than the 2.6-kb transcript and shows highest expression in the cerebellum. We also detected expression in lymphocyte RNA derived from the Tunisian individual with *ALS2* (Fig. 3b). *NarI*-based mutation analysis indicates that the expressed *ALS2* transcripts from affected individuals carry a homozygous 261delA mutation, which generates a novel *NarI* cutting site (Fig. 2d).

Deduced protein sequence of *ALS2*

Database searches show a number of interesting domains and motifs in the protein sequence deduced for human *ALS2*. A region in the amino-terminal half of *ALS2* is highly homologous to the regulator of chromosome condensation (RCC1)¹³ and the retinitis pigmentosa GTPase regulator (RPGR)¹⁷, including its functional structural motif, a seven-bladed propeller (Fig. 4b)¹⁸. RCC1 is a GEF for the nuclear GTP-binding protein Ran (Ras-related nuclear)¹³. A middle portion of *ALS2* contains a tandem organization of diffuse B-cell lymphoma (Dbl) homology¹⁹ and pleckstrin homology domains¹⁹ (Fig. 4a,c) that is a hallmark of GEFs for Rho (Ras-homologous member) GTPases¹⁹. In addition, a vacuolar protein sorting 9 (VPS9) domain, which is seen in a number of GEFs, including Vps9 (ref. 20), Rabex-5 (ref. 21) and RIN1 (ref. 22), is also found in the carboxy-terminal region (Fig. 4a; Web Fig. A). Two membrane occupation and recognition nexus (MORN) motifs²³ consisting of 23 amino acids and implicated in binding to plasma membranes are also noted in the region between the Dbl and pleckstrin homology domains and the VPS9 domain (Fig. 4a; Web Fig. A).

The mouse ortholog

We isolated the mouse ortholog of *ALS2*, designated *Als2*. Sequence analysis of *Als2* shows that it encompasses 6,349 nucleotides, with a single ORF that is 4,956 nucleotides long (124–5,079 nt) and is predicted to encode a 183-kD protein consisting of 1,651 amino acids. The entire ORF is well conserved between human and mouse (87% identity at DNA level; data not shown). Two transcripts with sizes similar to those in humans

were detected by northern blot analysis (data not shown). Deduced protein sequences for mouse *Als2* and human *ALS2* are conserved (91% identity, 94% similarity; Web Fig. B). To study the regional expression of the *Als2* transcript in mouse brain and spinal cord, we used *in situ* hybridization with riboprobes directed against a portion of the *Als2* cDNA. The *Als2* transcript is expressed to a variable degree in neuronal cells throughout the brain and spinal cord, particularly in hippocampus and dentate gyrus neurons, cerebellar Purkinje cells, cerebral cortex neurons and spinal gray matter, including anterior horn cells (Fig. 5). Prominent expression is also seen in neurons in the olfactory bulb, basal ganglia and cranial nuclei (data not shown).

Discussion

ALS2 is a recessive form of juvenile *ALS*^{6,10} and is heralded by symptoms in the first or second decade of life with progressive spasticity of the limbs and of the facial and pharyngeal muscles^{10,15}. Here we report the identification of two independent mutations in the same gene, *ALS2*, in

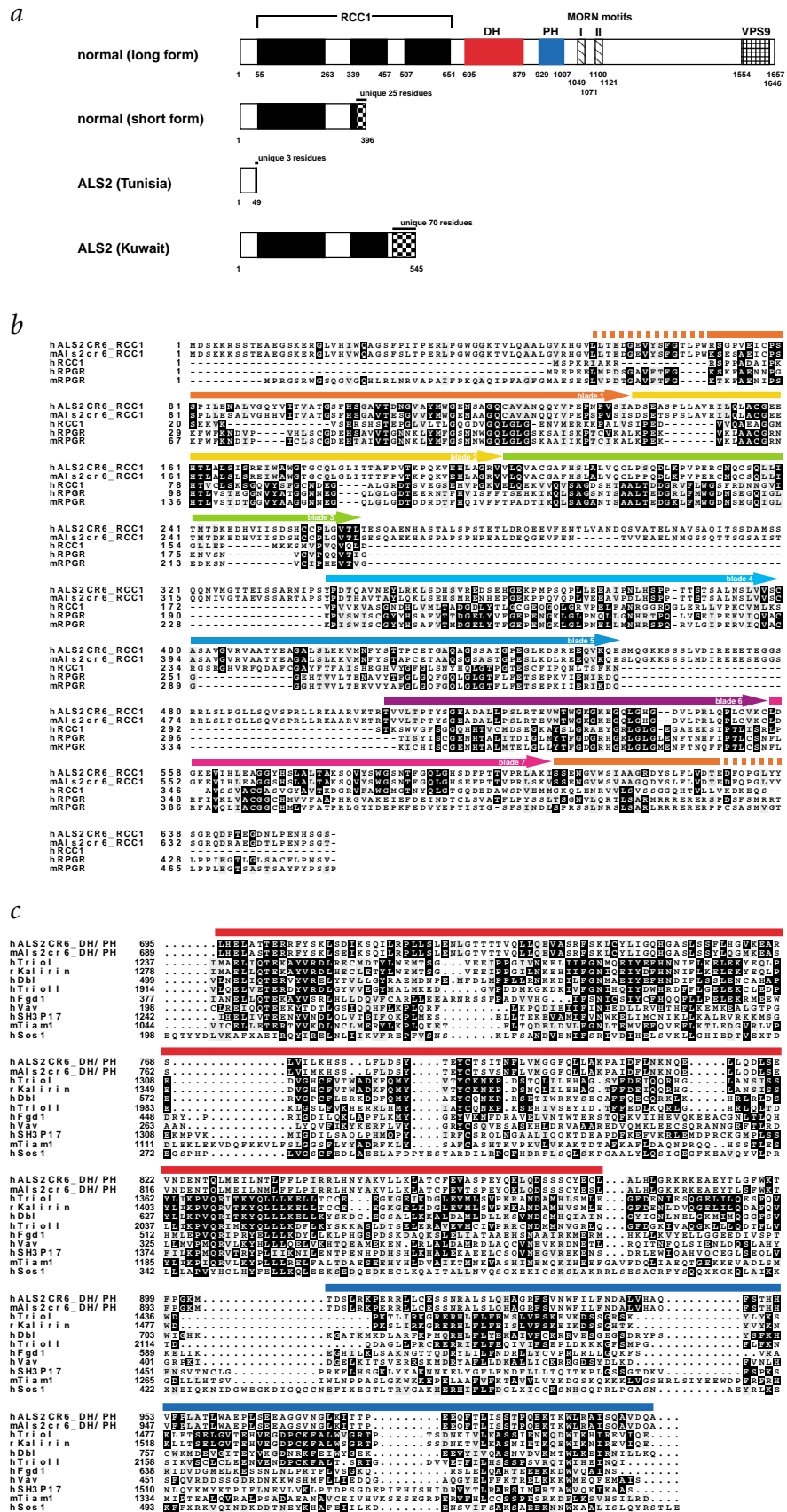
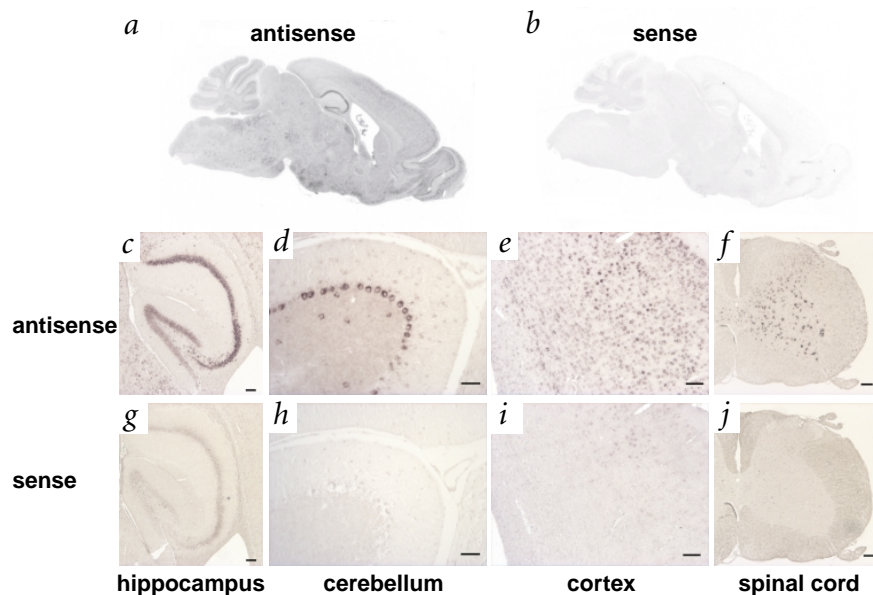


Fig. 4 Amino-acid sequence analysis. **a**, Schematic representation of the domains and motifs identified in the predicted normal and mutated *ALS2* proteins. Positions of unique 25 amino acid residues found in the short form of *ALS2* (starting from residue 372), 3 amino acid residues predicted from the Tunisian mutation (starting from residue 47) and 70 amino acid residues predicted from the Kuwaiti mutation (starting from residue 476) are shown. **b**, Multiple amino acid sequence alignment of the RCC1-repeat containing regions of human *ALS2*, *hALS2_RCC1*; mouse *Als2*, *mAls2_RCC1*; human *RCC1*, *hRCC1*; rat *RPGR*, *rRPGR*; mouse *RPGR*, *mRPGR*; and human *Sosl1*, *hSosl1*. The alignment is shown with the black and gray shadings representing identical and conserved amino acids, respectively. Position of each blade in a seven-bladed propeller for *RCC1* was drawn on top of the alignment according to previous data¹⁸. Sequences are numbered with the initiation codon (M) of each protein as no. 1. **c**, Multiple amino acid sequence alignment of DH-PH domains for: human *ALS2*, *hALS2_CR6_DH/PH*; mouse *Als2cr6*, *mAls2cr6_DH/PH*; the first DH-PH domain of human *Trio*, *hTrio1*; human *Dbl*, *hDbl*; human *Fgd1*, *hFgd1*; human *Vav*, *hVav*; human *SH3P17*, *hSH3P17*; mouse *Tiam1*, *mTiam1*; and human *Sosl1*, *hSosl1*. The alignment is shown with the black and gray shadings representing identical and conserved amino acids, respectively. Sequences are numbered with the initiation codon of each protein as no. 1.

corresponding to DH and PH domains, respectively. The alignment is shown with the black and blue bars on top of the alignment represent regions corresponding to DH and PH domains, respectively. The alignment is shown with the black and blue bars on top of the alignment represent regions corresponding to DH and PH domains, respectively. Sequences are numbered with the initiation codon of each protein as no. 1.

Fig. 5 Expression of *Als2* mRNA in adult mouse brain and spinal cord. **a,b**, Sagittal macro images of RNA/RNA *in situ* hybridization with antisense *Als2* riboprobe (**a**) and with sense-strand probe as a control (**b**). A definite signal in the brain is demonstrated including olfactory bulb, cerebral cortex, basal ganglia, cranial-nerve nuclei and cerebellum. **c,g**, Neurons in hippocampus and dentate gyrus. **d,h**, Purkinje cells in cerebellum. **e,i**, Neurons in cerebral cortex. **f,j**, Neurons in spinal gray matter including anterior horn cells are represented in a marked expression. Each scale bar represents 10 μ m in length.



unrelated families with ALS2. These deletion mutations result in frameshifts that generate premature stop codons. *ALS2* is expressed in various tissues and cells, including neurons throughout the brain and spinal cord, and encodes a protein containing multiple domains that have homology to RanGEF as well as RhoGEF. Deletion mutations are predicted to cause a loss of protein function, providing strong evidence that *ALS2* is the causative gene underlying ALS2.

The protein sequence deduced for human *ALS2* shows a number of interesting features relating to GEFs (Fig. 4a,c; Web Fig. A). First, the amino-terminal half of *ALS2* contains a region that is highly homologous to RCC1 (ref. 13) and RPGR (ref. 17), including its functional structural motif, a seven-bladed propeller (Fig. 4b)¹⁸. RCC1 acts as a GEF for Ran, an abundant small GTPase, and is implicated in nuclear transfer as well as chromatin condensation through the regulation of microtubule assembly²⁴. Although the RCC1 homologous domain in *ALS2* is interrupted by two intervening sequences, the blade sequences are not disrupted (Fig. 4b). Thus, *ALS2* could function as a GEF for Ran or Ran-related GTPases. Second, *ALS2* contains Dbp1 and pleckstrin homology domains (Fig. 4c)¹⁹. A tandem organization of Dbp1–pleckstrin homology domains is a hallmark of Rho GEFs¹⁹, which play important roles in various signaling cascades²⁵, neuronal morphogenesis²⁶, membrane transport or trafficking^{27,28} and organization of the actin cytoskeleton^{14,29}. In addition, a VPS9 domain is found in the carboxy-terminal region. The VPS9 domain is seen in a number of GEFs, including Vps9 (ref. 20), Rabex-5 (ref. 21) and RIN1 (ref. 22), and is known to mediate vacuolar protein sorting and endocytic trafficking. Two MORN motifs²³ consisting of 23 amino acids are also noted in the *ALS2* protein (Web Fig. A). A recent study on junctophilins that contain MORN motifs shows that this motif contributes to the binding to plasma membranes²³. GEFs are known to associate with GDP-bound forms of GTPases and accelerate GDP dissociation and GTP binding, thereby activating the GTPases. Taking this information together, it is possible that *ALS2* acts as a regulator/activator of particular GTPases and modulates the microtubule assembly, membrane organization and trafficking in cells, including neurons.

The 261delA mutation (Tunisian *ALS2*) in codon 46 causes disruption of the reading frame and is predicted to generate a truncated protein (5.4 kD), which consists of 49 amino acid residues with 3 new residues at the carboxy terminus (Fig. 4a; Web Fig. B). The 1548delAG mutation (Kuwaiti *ALS2*) in codon 475 also results in a frameshift that generates 70 new amino acids before a premature stop codon (Fig. 4a; Web Fig. B). Recent studies suggest that transcripts that contain premature translation

termination codons and code for nonfunctional or even harmful proteins are subject to nonsense-mediated mRNA decay (NMD), a conserved surveillance mechanism allowing the identification and elimination of imperfect mRNAs³⁰. It is therefore possible that the mutated *ALS2* mRNA could be degraded by NMD and does not serve as mRNA templates for protein translation. Based on our RT-PCR and northern blot analyses, however, the mutated *ALS2* transcript is indeed present in lymphocytes from an affected member of the Tunisian family (Figs. 2d,3b), suggesting that truncated *ALS2* can be produced from mutated transcripts (Fig. 4a). Given that these truncated proteins do not contain any of the putative functional domains of *ALS2* in complete form, the mutations are likely to be deleterious and cause a loss of function. Further, the predicted protein (58.3 kD) from the Kuwaiti *ALS2* family, which is longer than that of a short form of the normal *ALS2* protein, encodes only an incomplete RCC1 motif (Fig. 4a), indicating that the loss of function for the full-length *ALS2*CR6 might be associated with the *ALS2* phenotype. These findings also suggest that a short form of *ALS2* encoding nearly half of the RCC1 motif could be inactive or a functional modifier for the full-length *ALS2*.

Recent findings that ALS is associated with defects in axonal transport and cytoskeletal organization^{31,32} support the hypothesis that *ALS2* causes ALS, with defects in microtubule assembly, membrane organization and trafficking possibly resulting from the loss of modulatory function in Ran/Rho-related GTPases. Determination of the function of this new protein *in vitro* and *in vivo* is required to elucidate both the molecular pathogenesis of *ALS2* and the reason for the selective degeneration of motor neurons. Identification of a mouse ortholog of *ALS2* in this study is the first step towards the creation of *in vivo* model of ALS. In addition, isolation of specific upstream regulators and downstream effectors for *ALS2* will help unravel both the normal molecular cascades and the defective one that causes ALS2.

To our knowledge, *ALS2* is only the second FALS gene identified, the first being the copper-zinc superoxide dismutase (*SOD1*) gene in ALS. *SOD1* mutations are responsible for an autosomal dominant form with late onset (ALS1)³. The identification of *ALS2* has both clinical and biochemical implications. The characterization of a putative GTPase regulator in ALS will provide new avenues to explore the molecular pathogenesis not only of *ALS2* but also of other FALS^{3–5,8,9} and of SALS.



Methods

Families with ALS2. We analyzed 16 members of the Tunisian consanguineous family with ALS2¹⁰ and 7 members of the Kuwaiti family with ALS2¹⁵ (originally diagnosed as having primary lateral sclerosis)¹⁵. ALS2 is characterized by a progressive spasticity of limb and facial muscles accompanying distal amyotrophy of hands and feet. The age of onset of symptoms is 3–10 y¹⁰. Analysis of the genotypes in the polymorphic DNA markers in conjunction with the clinical data clearly indicates that ALS2 is an autosomal recessive disease, and its genetic locus has been mapped to chromosome 2q33 (refs. 6,7).

Transcript map. To identify the transcribed DNA sequences mapped within the candidate region, we searched the public databases in Genome Data Base (<http://gdbwww.gdb.org>) and UniGene at The National Center for Biotechnology Information (<http://www.ncbi.nlm.nih.gov>). Genomic DNA sequences overlapping the ALS2 candidate interval were retrieved from the 'nr' or 'htgs' database at GenBank, and were used as queries for BLAST search³³ against the dbEST. We also used RT-PCR, 5'-RACE and cDNA library screening to isolate the full-length transcripts. We sequenced purchased EST clones (Research Genetics) to determine their entire insert sequences. We sequenced double-stranded DNA by dideoxy sequencing using the BigDye Terminator Cycle Sequencing kit (ABI) and the ABI377 DNA sequencer. We aligned DNA sequences obtained from EST data, PCR products and cDNA clones, and established putative nonoverlapping transcriptional units. We then mapped each unit onto the physical map using a PCR-based method.

Exon identification. To define the intron/exon organizations of the transcribed sequences, we compared the cDNA sequences with the genomic DNA sequence data published in the GenBank database using BLAST³³ and Sequencher Version 3.0 (Gene Codes) as previously described^{11,12}.

PCR. We carried out PCR amplification of the region containing both exons and intron-exon boundaries (exon-PCR) in candidate genes. Genomic DNA (50 ng) was subjected to PCR amplification using *ExTaq* polymerase (Takara) and 35 cycles of 15 s at 95 °C, 30 s at 60 °C and 30 s at 72 °C. To detect the aberrant forms of transcripts, we carried out RT-PCR on total RNA from lymphocytes of four affected individuals and two carriers in the family with ALS2 using the SuperScript preamplification system (Invitrogen) according to the supplier's recommendations. We purchased total RNA extracted from normal human brain from Clontech for control RT-PCR. We designed oligonucleotide primers for these PCR reactions using Primer 3.0 (<http://www-genome.wi.mit.edu>).

Mutational analysis. To detect DNA sequence variations in exons or at intron-exon boundaries, we carried out DNA sequencing of the exon-PCR products. We compared DNA sequences obtained from affected patients, carriers and normal individuals in conjunction with the sequence data in public databases, and identified the nucleotide variations.

We carried out genotyping for the 261delA variant that creates a new *NarI* site in ALS2 by PCR amplification of exon 3 or RT-PCR amplification of exons 2–4, followed by restriction digestion with *NarI*. Forward and reverse primers for exon 3 PCR are 5'-CCTAGTCATCCATGTGCTGG-3' and 5'-TCCCATACCTGACCTTCCAC-3', respectively. Forward and reverse primers for exon 2–4 RT-PCR are 5'-CTTGATAGACTTTCTGTAAAGAAG-3' and 5'-GGCTACTTGGACAAATCTCCACTG-3', respectively. We separated the *NarI*-digested products on 1.5% agarose gels.

We carried out genotyping for the 1548delAG variant using a DHPLC WAVE system (Transgenomics). We sequenced samples that displayed abnormal retention times in both directions using a Thermosequenase ³³P cycle sequencing kit (United States Biochemical). We resolved sequences on 6% polyacrylamide gels and read them after exposure to autoradiography film.

Northern blot analysis. We separated 10 µg of total RNA extracted from normal brain and 20 µg of those from lymphocytes of affected and unaffected individuals and blotted it onto the nylon membrane. We then hybridized several human adult tissue northern blots (Clontech) and the total RNA blot with [³²P]dCTP-labeled exon 4 of ALS2CR6 or human β-actin cDNA in PerfectHyb hybridization solution (Toyobo) at 68 °C. We washed membranes with 0.1×SSC containing 1% SDS at 65 °C and exposed them to X-ray film (Bio-MAX, Kodak).

In situ hybridization of RNA. We prepared antisense and sense cRNA probes from two mouse cDNA clones, m2-as and m2-s, that carried the portion of mouse *Als2cr6* cDNA (1,732–2,685 nt; 954 bp) in pCR2.1 vector (Invitrogen) with opposite orientations, in an *in vitro* transcription reaction incorporating digoxigenin-labeled UTP with T7 RNA polymerase according to the manufacturer's protocol (Roche). Methods for sample preparations and *in situ* hybridization are described elsewhere³⁴.

Database searches. We compared DNA and amino acid sequences with non-redundant nucleotide and protein sequence databases using BLASTN and BLASTP, respectively³³. We identified protein motifs and domains using the MOTIF server at GenomeNet Japan (<http://www.genome.ad.jp>), BCM search launcher (<http://searchlauncher.bcm.tmc.edu>) and CD-Search at NCBI (<http://www.ncbi.nlm.nih.gov>). We carried out the multiple protein sequence alignment using ClustalW 1.80 (<http://www.genome.ad.jp>) and displayed it using BOXSHADE (http://www.ch.embnet.org/software/BOX_form.html).

Genbank/EMBL/DDBJ accession numbers. ALS2CR4, AB053301; ALS2CR5/MPP4 variant (long), AB053302; ALS2CR5/MPP4 variant (short), AB053303; ALS2CR5/MPP4 alternative form, AB053304; ALS2 (ALS2CR6; long form), AB053305; ALS2 (ALS2CR6; short form), AB053306; *Als2cr6* (mouse ortholog), AB053307; ALS2CR7, AB053308; ALS2CR8 (long form), AB053309; ALS2CR8 (short form), AB053310; ALS2CR9, AB053311; ALS2CR10, AB053312; ALS2CR11, AB053313; ALS2CR12, AB053314; ALS2CR13, AB053315; ALS2CR14, AB053316; ALS2CR15, AB053317; ALS2CR16, AB053318; ALS2CR17, AB053319; ALS2CR18, AB053320; ALS2CR19, AB053321.

Note: supplementary information is available on the Nature Genetics web site (http://genetics.nature.com/supplementary_info/).

Acknowledgments

We thank the patients and other members of the ALS2 families for participating in this study; A.E. MacKenzie, R.G. Korneluk, I. Kanazawa, J.-C. Barbot and J.-C. Kaplan for providing control DNA samples; D. Rochefort for technical support; and all the members of our laboratories for helpful discussion and suggestions. This work was funded by the Japan Science and Technology Corporation, the Canadian Genetic Diseases Network, the Centre for Molecular Medicine and Therapeutics, the Nakabayashi Trust For ALS Research, the Japan Brain Foundation, the Grant-in-Aid for Scientific Research Priority Areas for the Ministry of Education, Science, Sports, and Culture (Japan), the Canadian Institute for Health Research, the Muscular Dystrophy Association (USA), the Amyotrophic Lateral Sclerosis Association, the National Institute for Neurological Disease (USA), National Institute for Aging (USA), Angel Fund for ALS Research (Boston, USA), Project ALS (New York, USA), Pierre L. DeBourgnicht ALS Research Foundation and Al-Athel ALS Foundation. M.R.H. is a holder of a Canada Research Chair. G.A.R. is supported by the Canadian Institute of Health Research. S.W.S. is a Scholar of the Medical Research Council of Canada. J.-E.I. is a scientific director of NeuroGenes/International Cooperative Research Project/Japan Science and Technology Corporation.

Received 5 June; accepted 9 July 2001.

- Siddique, T., Nijhawan, D. & Hentati, A. Molecular genetic basis of familial ALS. *Neurology* **47**, 527–535 (1996).
- Siddique, T. et al. Linkage of a gene causing familial amyotrophic lateral sclerosis to chromosome 21 and evidence of genetic-locus heterogeneity. *N. Engl. J. Med.* **324**, 1381–1384 (1991).
- Rosen, D.R. et al. Mutations in Cu/Zn superoxide dismutase gene are associated with familial amyotrophic lateral sclerosis. *Nature* **362**, 59–62 (1993).
- Chance, P.F. et al. Linkage of the gene for an autosomal dominant form of juvenile amyotrophic lateral sclerosis to chromosome 9q34. *Am. J. Hum. Genet.* **62**, 633–640 (1998).
- Blair, I.P. et al. A gene for autosomal dominant juvenile amyotrophic lateral sclerosis (ALS4) localizes to a 500-kb interval on chromosome 9q34. *Neurogenetics* **3**, 1–6 (2000).
- Hentati, A. et al. Linkage of recessive familial amyotrophic lateral sclerosis to chromosome 2q33–q35. *Nature Genet.* **7**, 425–428 (1994).
- Hosler, B.A. et al. Refined mapping and characterization of the recessive familial amyotrophic lateral sclerosis locus (ALS2) on chromosome 2q33. *Neurogenetics* **2**, 34–42 (1998).
- Hentati, A. et al. Linkage of a commoner form of recessive amyotrophic lateral sclerosis to chromosome 15q15–q22 markers. *Neurogenetics* **2**, 55–60 (1998).



9. Hosler, B.A. et al. Linkage of familial amyotrophic lateral sclerosis with frontotemporal dementia to chromosome 9q21-q22. *JAMA* **284**, 1664–1669 (2000).
10. Ben Hamida, M., Hentati, F. & Ben Hamida, C. Hereditary motor system diseases (chronic juvenile amyotrophic lateral sclerosis). *Brain* **113**, 347–363 (1990).
11. Hadano, S. et al. A yeast artificial chromosome-based physical map of the juvenile amyotrophic lateral sclerosis (ALS2) critical region on human chromosome 2q33-q34. *Genomics* **55**, 106–112 (1999).
12. Hadano, S. et al. Cloning and characterization of three novel genes, *ALS2CR1*, *ALS2CR2*, and *ALS2CR3*, in the juvenile amyotrophic lateral sclerosis (ALS2) critical region at chromosome 2q33-q34: candidate genes for ALS2. *Genomics* **71**, 200–213 (2001).
13. Ohtsubo, M. et al. Isolation and characterization of the active cDNA of the human cell cycle gene (*RCC1*) involved in the regulation of onset of chromosome condensation. *Genes Dev.* **1**, 585–593 (1987).
14. Luo, L. Rho GTPases in neuronal morphogenesis. *Nature Rev. Neurosci.* **1**, 173–180 (2000).
15. Lerman-Sagie, T., Filiano, J., Smith, D.W. & Korson, M. Infantile onset of hereditary ascending spastic paralysis with bulbar involvement. *J. Child Neurol.* **11**, 54–57 (1996).
16. Nagase, T., Kikuno, R., Nakayama, M., Hirose, M. & Ohara, O. Prediction of the coding sequences of unidentified human genes. XVIII. The complete sequences of 100 new cDNA clones from brain which code for large protein in vitro. *DNA Res.* **7**, 273–281 (2000).
17. Meindl, A. et al. A gene (*RPGR*) with homology to the *RCC1* guanine nucleotide exchange factor is mutated in X-linked retinitis pigmentosa (RP3). *Nature Genet.* **13**, 35–42 (1996).
18. Renault, L. et al. The 1.7 Å crystal structure of the regulator of chromosome condensation (*RCC1*) reveals a seven-bladed propeller. *Nature* **392**, 97–101 (1998).
19. Soisson, S.M., Nimnual, A.S., Uy, M., Bar-Sagi, D. & Kuriyan, J. Crystal structure of the Dbl and pleckstrin homology domains from the human Son of sevenless protein. *Cell* **95**, 259–268 (1998).
20. Hama, H., Tall, G. G. & Horazdovsky, B.F. Vps9p is a guanine nucleotide exchange factor involved in vesicle-mediated vacuolar protein transport. *J. Biol. Chem.* **274**, 15284–15291 (1999).
21. Horiuchi, H. et al. A novel Rab5 GDP/GTP exchange factor complexed to Rabaptin-5 links nucleotide exchange to effector recruitment and function. *Cell* **90**, 1149–1159 (1997).
22. Tall, G.G., Barbieri, M.A., Stahl, P.D. & Horazdovsky, B.F. Ras-activated endocytosis is mediated by the Rab5 guanine nucleotide exchange activity of RIN1. *Dev. Cell* **1**, 73–82 (2001).
23. Takeshima, H., Kamazaki, S., Nishi, M., Iino, M. & Kangawa, K. Juncophilins: a novel family of junctional membrane complex proteins. *Mol. Cell* **6**, 11–22 (2000).
24. Carazo-Salas, R.E. et al. Generation of GTP-bound Ran by RCC1 is required for chromatin mitotic spindle formation. *Nature* **400**, 178–181 (1999).
25. Barrett, K., Leptin, M. & Settleman, J. The Rho GTPase and a putative RhoGEF mediate a signaling pathway for the cell shape changes in *Drosophila* gastrulation. *Cell* **91**, 905–915 (1997).
26. Martijn, F.B.G. et al. Identification of a novel, putative Rho-specific GDP/GTP exchange factor and a RhoA-binding protein: control of neuronal morphology. *J. Cell Biol.* **137**, 1603–1613 (1997).
27. Roepman, R. et al. The retinitis pigmentosa GTPase regulator (RPGR) interacts with novel transport-like proteins in the outer segments of rod photoreceptors. *Hum. Mol. Genet.* **9**, 2095–2105 (2000).
28. Alam, M.R. et al. Kalirin, a cytosolic protein with spectrin-like and GDP/GTP exchange factor-like domains that interacts with peptidylglycine alpha-amidating monooxygenase, an integral membrane peptide-processing enzyme. *J. Biol. Chem.* **272**, 12667–12675 (1997).
29. Hall, A. Rho GTPases and the actin cytoskeleton. *Science* **279**, 509–514 (1998).
30. Culbertson, M.R. RNA surveillance. Unforeseen consequences for gene expression, inherited genetic disorders and cancer. *Trends Genet.* **15**, 74–80 (1999).
31. Collard, J.-F., Côté, F. & Julien, J.-P. Defective axonal transport in a transgenic mouse model of amyotrophic lateral sclerosis. *Nature* **375**, 61–64 (1995).
32. Williamson, T.L. & Cleveland, D.W. Slowing of axonal transport is a very early event in the toxicity of ALS-linked SOD1 mutants to motor neurons. *Nature Neurosci.* **2**, 50–56 (1999).
33. Altschul, S.F. et al. Gapped BLAST and PSI-BLAST: a new generation of protein database search programs. *Nucleic Acids Res.* **25**, 3389–3402 (1997).
34. Matsumoto, K. et al. Neuronal apoptosis inhibitory protein (NAIP) may enhance the survival of granulosa cells thus indirectly affecting oocyte survival. *Mol. Reprod. Dev.* **54**, 103–111 (1999).